

Towards development of a statistical framework to evaluate myotonic dystrophy type 1 mRNA biomarkers in the context of a clinical trial

Adam Kurkiewicz^{1*}, Anneli Cooper³✉, Emily McIlwaine³, Sarah A. Cumming³, Berit Adam³, Ralf Krahe⁴, Jack Puymirat⁵, Benedikt Schoser⁶, Lubov Timchenko⁷, Tetsuo Ashizawa⁸, Charles Thornton⁹, Simon Rogers²✉, John McClure¹✉, Darren G Monckton³✉

1 Institute of Cardiovascular and Medical Sciences, University of Glasgow, Glasgow, United Kingdom

2 School of Computing Science, University of Glasgow, Glasgow, United Kingdom

3 Institute of Molecular Cell and Systems Biology, College of Medical, Veterinary and Life Sciences, University of Glasgow, Glasgow, United Kingdom

4 Department of Genetics, University of Texas, MD Anderson Cancer Center, Houston, TX, USA

5 Laboratory of Human Genetics, CHUL Medical Research Centre, University of Laval, Quebec City, QC, Canada

6 Friedrich Baur Institute, Department of Neurology, Ludwig Maximilians University, Munich, Germany

7 Department of Pediatrics, Division of Neurology, Cincinnati Children's Hospital, University of Cincinnati, College of Medicine, Cincinnati Ohio, USA

8 VA Medical Center, Houston, Texas, USA

9 University of Rochester, Medical Center School of Medicine and Dentistry, Rochester, New York, USA

✉These authors contributed equally to this work.

✉Institute of Biodiversity, Animal Health and Comparative Medicine, University of Glasgow, Glasgow, United Kingdom

* Adam.Kurkiewicz@glasgow.ac.uk

Abstract

Myotonic dystrophy type 1 (DM1) is a rare genetic disorder, characterised by muscular dystrophy, myotonia, and other symptoms. DM1 is caused by the expansion of a CTG repeat in the 3'-untranslated region of *DMPK*. Longer CTG expansions are associated with greater symptom severity and earlier age at onset. The primary mechanism of pathogenesis is thought to be mediated by a gain of function of the CUG-containing RNA, that leads to *trans*-dysregulation of RNA metabolism of many other genes. Specifically, the alternative splicing (AS) and alternative polyadenylation (APA) of many genes is known to be disrupted. In the context of clinical trials of emerging DM1 treatments, it is important to be able to objectively quantify treatment efficacy at the level of molecular biomarkers. We show how previously described candidate mRNA biomarkers can be used to model an effective reduction in CTG length, using modern high-dimensional statistics (machine learning), and a blood and muscle mRNA microarray dataset. We show how this model could be used to detect treatment effects in the context of a clinical trial.

Introduction

Myotonic dystrophy type 1

Myotonic dystrophy type 1 (DM1) is an autosomal dominant trinucleotide repeat disorder, caused by an expanded CTG repeat in the 3' UTR of the *dystrophia myotonica protein kinase* (*DMPK*) gene [1]. Transcription of *DMPK* in affected individuals produces a toxic, GC-rich mRNA molecule, which results in dysregulation of several RNA binding factors, including proteins MBNL1, MBNL2, MBNL3, CELF1 (CUGBP1), HNRNPH1 and STAUF1 (Staufen1) [2,3]. The pathomechanism of the dysregulation of splicing factor MBNL1 is perhaps best understood, with MBNL1 sequestration to the toxic *DMPK* RNA product resulting in alternative splicing defects of pre-mRNAs of multiple genes, including the chloride channel (*CLCN1*), brain microtubule-associated tau (*MAPT*) and insulin receptor (*INSR*) [4]. Such alternative splicing (AS) defects are generally believed to be a major contributing factor of clinical symptoms of DM1, such as myotonia (*CLCN1*) or abnormal glucose response (*INSR*),

and have been postulated to play a role in cardiac conduction defects (*RYR2*, *SERCA2*, 15
TNNT2) [5]. AS defects may underlie other clinical symptoms of DM1, including muscle 16
wasting, cataracts, hypersomnia, gastrointestinal abnormalities, as well as premature 17
baldness and testicular atrophy in males [2, 6]. The severity of symptoms is positively 18
correlated with CTG repeat length [2]. 19

The toxic *DMPK* transcript in DM1-affected individuals has been identified as an 20
active target for therapeutic intervention [7], and it is expected that breakdown of the 21
toxic mRNA will result in at least partial reversal of DM1-induced AS changes and 22
other known and unknown DM1-induced biomolecular pathologies. 23

Spliceopathy of DM1 is an active area of research, with novel splicing defects being 24
continuously reported. Nakamori *et al.* [8] identified a set of 41 genes, which are 25
mis-spliced in DM1, suggesting these genes as potential biomarkers of DM1. Batra *et* 26
al. [9] identified 80 genes, whose expression indicates disrupted APA, reusing the 27
(human) dataset of Nakamori *et al.* and using other datasets, including data from 28
mouse models. 29

Predictors in genetics research 30

A widespread paradigm in biological and clinical research is the case-control study, 31
using frequentist statistics tools focusing on hypothesis testing (inference). Examples of 32
such designs include Genome Wide Association Studies (GWAS) [10], placebo and 33
active control clinical trial designs [11], non-inferiority designs [12] or heredity designs 34
based on twin studies. It is reported that designs of as many as 70% of studies 35
published in leading medical journals use at most the following three statistical tests as 36
part of their design: Student's t-test, Fisher's exact test, and the Chi-square test [13]. 37

A possible alternative to the focus on hypothesis testing is building predictors or 38
classifiers, which produce a numerical estimate of a given trait (height, size of the DM1 39
trinucleotide expansion) or effect size, predict participant's category (such as 40
affected/unaffected), or estimate the effect size of the treatment, given a set of 41
independent variables (e.g. genotypes, mRNA profiles, *etc.*). If necessary, the efficacy of 42
these predictors/classifiers can be evaluated using traditional frequentist tools, such as 43
p-values. 44

Predictors have been successfully applied in genetics research. For example, Lello *et al.* [14] report predicting human height from genotype data, obtained using human Single Nucleotide Polymorphism (SNP) microarrays, to within a few centimeters for most participants in their sample. This level of accuracy is achieved due to a very large sample size of nearly half a million individuals. A review by Van Raden *et al.* [15] reports ability to predict dairy output of certain cattle breeds with R^2 of 49%, using non-linear models based on SNP microarrays. The work of Azencott *et al.* [16] allows one to incorporate prior information about biological networks into the predictive model, increasing prediction accuracy. In one of the direct motivations behind our research here, Lee *et al.* [17] report being able to predict most of Huntington disease trinucleotide repeat size using mRNA profiling of lymphoblastoid cell lines. Here, we demonstrate a further application of predictors in genetics research, by constructing a predictor, which can produce a numerical estimate of a participant's DM1 CTG repeat length (measured from blood) from an mRNA profile (obtained from muscle), and demonstrate its usefulness in the context of a hypothetical clinical trial of a DM1 treatment.

Prior identification of alternative splicing and alternative polyadenylation events in muscles of DM1-affected individuals

Our primary reference is the work of Nakamori *et al.* [8], who identified 42 genes exhibiting AS defects in DM1. Briefly, the methodology of the study was as follows: muscle tissue (patients: four biceps, two quadriceps, one tibialis anterior, one diaphragm; controls: eight vastus lateralis) were sampled post-mortem from eight DM1 affected individuals and eight unaffected controls. Selection of the postmortem DM1 samples were based on high integrity of RNA present in the sample and presence of splicing misregulation of *INSR* and *AP2A1*, and then compared to quadriceps biopsy samples from eight healthy controls.

mRNA was extracted from the samples, purified and hybridized to GeneChipTM Human Exon 1.0 ST microarrays. Putative AS defects were identified using a mixture of existing methods, such as Affymetrix's PLIER, DABG and Alternative Transcript Analysis Methods for Exon Arrays, and new methods proposed and described by the authors. Identified putative defects were validated using RT-PCR in 50 DM1 subjects,

yielding 42 genes with confirmed AS defects.

Nakamori *et al.* report several technical obstacles with this approach, with the initial version of their pipeline suffering from as many as 80% putative AS defects failing to replicate with Reverse Transcription-PCR. Further analysis suggested that this occurred when “signal intensity for the entire transcript or a particular exon was low”, “overall expression of a transcript was strongly up- or down- regulated in DM1 relative to normal controls”, or “signal intensity of an exon was inappropriately high relative to other exons in the same transcript” [8].

Batra *et al.* [9] re-used the dataset of Nakamori *et al.* [8] and used similar techniques to filter down the data, in a search for genes with dysregulated APA. Their selection criteria focused on probesets with over 2-fold change in DM1 or DM2 vs. unaffected controls, excluding genes that were represented by ≤ 5 probesets, retrogenes and non-protein coding genes, which resulted in pre-selection of 438 probesets. The authors performed visual inspection of all pre-selected probesets identifying 123 APA events belonging to 80 genes.

Evaluating Potential Biomarkers of DM1

We propose that predictors are a suitable statistical tool, which can find applications in DM1 research and clinical practice. As described before, DM1 case/control status [8, 9] leaves a discernible pattern in the mRNA profiles of muscle samples. In this research, rather than to work with the DM1 status as a binary variable, we look at DM1 as a spectrum disease, severity of which is quantified by the length of the DM1 CTG repeat in any individual patient. We propose that it is possible to capture the effect, which the length of this repeat has on mRNA expression in muscle into a simple statistical model, based on linear regression. Using the model we can predict the size of the DM1 CTG repeat from the mRNA profile significantly better than a random predictor. We propose that the model can serve as a valuable tool in evaluating efficacy of any treatment for DM1 as such treatment enters pre-clinical or clinical trials, by enabling investigators to directly quantify the treatment effect as measured by effective reduction of DM1 CTG repeat length.

We would like to stress here that “effective reduction” in the case of most candidate

treatments will not be an actual reduction in the repeat length (with notable exception 105 of candidate treatments based on gene editing). Rather, an “effective reduction” is a 106 reduction of “effective repeat length”, i.e. repeat length as judged by the degree of 107 splicing changes. This can be demonstrated with an example of a patient with a certain 108 pre-treatment repeat length, and both physiological and molecular symptoms 109 characteristic for that repeat length. If such patient were to undergo an effective 110 treatment we would expect these symptoms to be partially reversed, and our predictive 111 framework to predict a shorter repeat length than the patient’s actual repeat length. 112 Subject to correctness of our understanding of the molecular pathophysiology of the 113 splicing changes, which we rely on to predict the effective repeat length, we expect that 114 the reversal of the splicing changes would occur immediately after the release of 115 inactivated AS and APA factors, such as MBNL1. This release should in turn happen 116 immediately after a candidate therapeutic were to reach a clinically significant level in 117 the relevant tissue. We expect this to happen on a timescale of days to weeks, unlike 118 the reversal of physiological symptoms, which we would expect to happen on longer 119 timescales. 120

Materials and methods 121

The dataset 122

As part of the *Dystrophia Myotonica* Biomarker Discovery Initiative (DMBDI) a dataset 123 was obtained from 35 participants, including 31 DM1 cases and four unaffected controls. 124 All DM1 cases in this research were heterozygous for the abnormally expanded CTG 125 repeat. The mode of the length of the DM1 CTG expansion (Modal Allele Length, 126 MAL) was determined by small-pool PCR of blood DNA for 35/36 patients [18]. For 127 this work we did not attempt to measure the repeat length from muscle, due to a very 128 high degree of repeat instability in muscle cells [3] and associated difficulties in its 129 experimental measurement. One patient refused blood donation. For each of the 35 130 blood-donating patients mRNA expression profiling of blood was performed using 131 Affymetrix GeneChip™ Human Exon 1.0 ST microarray. For 28 of 36 patients a 132 successful quadriceps muscle biopsy was obtained. The muscle tissue was mRNA 133

profiled using the same type of microarray. In total, a complete set of samples (blood and muscle) was obtained for 27 of 36 patients. mRNA profiling was carried out by the GeneLogic service lab (on a fee-for-service basis) using standard Affymetrix hybridisation protocol.

Principal Component Analysis (PCA) was performed on both blood and muscle profiles, and visual inspection was carried out to detect the presence of outliers. Zero outliers in the blood batch and four outliers in the muscle batch were identified and expression profiling was repeated for these patients. For the analysis we used only the repeated profiles.

It should be noted that our dataset differs from the dataset collected by Nakamori *et al.* in the following ways:

1. We did not perform confirmatory RT-PCR analyses.
2. Our dataset includes both blood and muscle tissue samples.
3. The number of mRNA-profiled participants is about twice the size of the discovery dataset of Nakamori *et al.*, however, we did not perform a follow-up validation study.
4. Unlike Nakamori *et al.* we have additional information to participant's case-control status, specifically, the mode of the CTG repeat length from blood (MAL). We also estimate the repeat length at birth (Progenitor Allele Length, PAL) using a previously developed method [19].
5. We sample from the same muscle group (quadriceps), as opposed to from a wide range of muscle groups (biceps, quadriceps, tibialis anterior, diaphragm, vastus lateralis) for all study participants, which eliminates a potentially important confounding effects.
6. All our participants are alive at the time of sample collection, which eliminates another potential confounder, but other potential confounders still remain, see [Limitations](#).

The dataset is deposited to Array Express with accession number E-MTAB-7983.

Affymetrix GeneChip™ Human Exon 1.0 ST microarray

The microarray chip used was the Affymetrix GeneChip™ Human Exon 1.0 ST microarray, which contains over 5 million probes, *i.e.* short cDNA sequences, which target transcribed regions with high specificity. Each probe in the HuEx chip contains precisely 25 nucleotides. Consequently, transcribed regions of interest, which are shorter than 25 nucleotides, for example some of the short exons, are not targeted. This is an important limitation in the context of DM1, as some AS events previously described in DM1, such as AS of exon 5 in cardiac troponin T (*TNNT2*) [20] cannot be detected.

Each continuous section of DNA can be targeted by a collection of up to four probes, referred to as probeset. DNA sections targeted by the chip include known and suspected coding exons in known and suspected genes, as well as non-coding genomic features, including 5' and 3' UTRs, and various other types of transcribed or hypothetically transcribed DNA (miRNA, rRNA, pseudo-genes, *etc.*). All probes targeting such a region belong to a single probeset. Probesets are further grouped into transcription clusters, which correspond to the entire genes.

Data preparation and analysis

We designed and built a pipeline, programmed in Python, which has the following data preparation capabilities: Reading raw Affymetrix CEL v4 files (peer reviewed and merged into Biopython [21,22]); quantile normalisation and log2 transformation of intensity data; strict annotation of Affymetrix probes using GENCODE v26 lift 37 through selecting probes corresponding to annotated GENCODE transcripts of type “protein_coding”, annotated genes of type “protein_coding” and exons of type “CDS” or “UTR”. Appendix S1 Appendix gives full source code, user manual and additional explanation of each step of this pipeline.

The pipeline’s final output are two directories: “experiment_muscle” and “experiment_blood”, each containing 19,826 files, whose filenames correspond to HGNC gene names. The following is a two-line excerpt from one of such files, “experiment_blood/TNNI1”. Data for several patients has been removed to enhance clarity:

gene_name	probeset_id	seq5to3plus	chrom	strand
-----------	-------------	-------------	-------	--------

→	genecode_left	genecode_right	x	y	193
→	patient_111747589		patient_117440822	...	194
→	patient_896445336				195
TNNI1	2450836	TGGCCTGTGCGCTCGCCGTAGACTGC		chr1	—
→	201390827		201390851	195	793
→	6.69115092487	6.44442470429	...	6.86989190909	198
					199

In each file, the first row is a header containing tab-separated names of data or metadata types contained in a given column. Below we give a brief description of some of the data or metadata types:

- seq5to3 – unlike Affymetrix we always report the sequence in 5' to 3' direction, and always with regards to the plus strand, even if the coding sequence is contained on the minus strand.
- genecode.left, genecode.right – these are genomic coordinates as reported by a reference assembly (GRCh37). Following convention, first coordinate is 1-based, and coordinates are left-, right- inclusive.
- x, y give the x and the y coordinates of probes on the chip.
- patient_* – these are quantile normalised and log2-transformed intensities at the given probe for the given study participant.

Each subsequent row contains data and metadata for a single probe.

We develop a predictive model, which closely follows that of Lee *et al.* [17]. We work with pre-selected sets of genes that act as candidate biomarkers. For this purpose, we look at the following collections of genes:

1. A previously identified selection of genes, listed in [S2 Appendix](#) and identified by Nakamori et al. [8] as genes whose AS is disrupted in DM1. We codename these genes “DM1-AS”.
2. A previously identified selection of genes, listed in [S3 Appendix](#) and identified by Batra et al. [9] as genes whose AP is disrupted in DM1. We codename these genes “DM1-APA”. The overlap of this list of genes with DM1-AS is a list of two genes: LDB3, MBNL2.

3. A single gene (which also belongs to DM1-APA), Troponin I1, slow skeletal type, 223
TNNI1. We codename this single-gene collection “TNNI1”. The gene was chosen 224
post-hoc. 225
4. All human genes, as identified in data preparation step. We codename this 226
collection “ALL”. 227

Then we execute eight separate statistical analyses (four muscle and four blood 228
analyses), based on these groups of genes. Each analysis was carried out as follows: 229

1. We randomly split our data into two sets, the training and the testing set, each 230
containing 70% and 30% of participants respectively. We restricted our analysis 231
only to genes, which belonged to a particular group of genes being studied 232
(DM1-APA, DM1-AS, TNNI1, ALL) 233
2. Following Lee *et al.*, we select (up to) 500 probes whose intensities across all 234
patients in the training set are most correlated with their corresponding MAL. We 235
work at the level of individual probes, which allows us to circumvent issues around 236
GC-correction and probeset aggregation. Probe data are fed directly into the 237
model. 238
3. Again using the training set, we trained a 2-dimensional Partial Least Squares 239
Regression (PLSR) model on selected probes as features and corresponding MAL 240
as the model output, which we later used to predict MAL in the testing set, again 241
following Lee *et al.*. 242
4. We repeated steps 1 to 3 10,000 times. 243
5. We report coefficient of determination (R^2) of the predicted MAL with the 244
measured MAL across all folds obtained in step 4. 245
6. We simulated a distribution of R^2 of a random predictor, and obtained a p-value 246
for the prediction of R^2 in step 5. 247

To confirm that any observed signal is not a by-product or an artifact of the 248
mathematical model used, or its implementation, we carried out the same kind of 249
analysis using three other mathematical models: 250

1. lasso 251
2. random forest regression 252
3. linear regression 253

To relate our findings to a potential clinical setting, we present power analysis 254
relating various potential treatment effect sizes to their detectability in future clinical 255
trials. The power analysis was performed as follows: 256

1. We simulated the distribution of MAL prediction error for the best predictor. 257
2. We simulated the distribution of MAL post-treatment, with the assumption that 258
MAL would be reduced by 10%, 20% or 50%, which correspond to, respectively, 259
small, medium and large treatment effect size. 260
3. We established the rejection region for a null hypothesis of “no treatment effect” 261
at $\alpha = 0.05$. 262
4. We simulated the power, $(1 - \beta)$, for studies involving 10 to 200 participants, in 263
increments of 10 participants. 264

Results & Discussion 265

Performance of PLSR-based MAL predictors in muscle and 266 blood 267

Using our predictive model based on PLSR and a selection of candidate biomarkers: 268
DM1-AS; DM1-APA; TNNI1 and ALL, we can report the following capabilities to 269
predict MAL from mRNA profiles. 270

In muscle we can detect strong signal for some of the selected candidate biomarker 271
sets, with the two strongest predictors, DM1-AS and TNNI1, giving us R^2 and p-values 272
equal to 0.289, 0.320 and 0.00434, 0.00249 respectively. All values of R^2 and p-values 273
are given in Table 1. In particular, DM1-AS looks promising as a set of biomarkers, 274
giving weight to the findings of Nakamori *et al.* [8]. 275

Based purely on numerical analysis of obtained results, one could declare TNNI1 as 276
the best predictor of MAL in muscle, but care must be taken, as we chose this 277

particular gene post-hoc and its true predictive value might have been influenced by 278 issues related to multiple hypotheses testing. An additional validation study would have 279 to be performed before drawing any conclusions on the performance of TNNI1 as a DM1 280 biomarker. 281

A safer belief can be assigned to the predictive value of “DM1-AS” and “DM1-APA” 282 as both sets of genes have been previously implicated in DM1 [9], and we can detect 283 strong signal from both sets of genes, with models based on these genes capturing 284 respectively 30% and 15% of MAL variance in our study group. 285

One has to note an interesting observation relating to the “curse of dimensionality” 286 and the performance of our PLSR-based model. Although TNNI1 is a subset of 287 DM1-APA, TNNI1 on its own is a much better predictor than DM1-APA, as increasing 288 the number of genes (features) increases the dimensionality of our data and worsens the 289 prediction delivered by the PLSR model. 290

A single run of 10,000 repetitions of a simulation can be visualised by plotting the 291 predicted value of MAL against the actual, adding a small amount of random noise on 292 the x-axis. For DM1-AS in muscle, such visualisation is given in Fig 1. 293

In blood we cannot detect significant signal for most candidate biomarkers, with R^2 294 not significantly respectively greater and lower than would be expected by chance, 295 except in one case, DM1-APA, whose R^2 and p-value are 0.15 and 0.0564 respectively. 296 Full R^2 and (uncorrected) p-values are given in Table 2. Poor performance of blood 297 data acting as a predictor of repeat length is perhaps not unexpected, as all candidate 298 biomarkers evaluated in this study are based on prior analyses of muscle data, and 299 might not be expressed, or only lowly expressed in blood, or that expression profiles 300 might be very different from expression profiles in muscle. Only DM1-APA can 301 potentially carry some predictive value, however, not as strongly as in muscle. 302

Table 1. 10000 repetitions of a simulation predicting MAL from muscle cross-validated with a testing set separate from the training set.

	DM1-AS	DM1-APA	TNNI1	ALL
R^2	0.289	0.150	0.320	0.084
p-value	0.00434	0.0470	0.00249	0.143

Table 2. 10000 repetitions of a simulation predicting MAL from blood cross-validated with a testing set separate from the training set.

	DM1-AS	DM1-APA	TNNI1	ALL
R ²	0.0465	0.106	0.0479	0.0465
p-value	0.213	0.0564	0.207	0.213

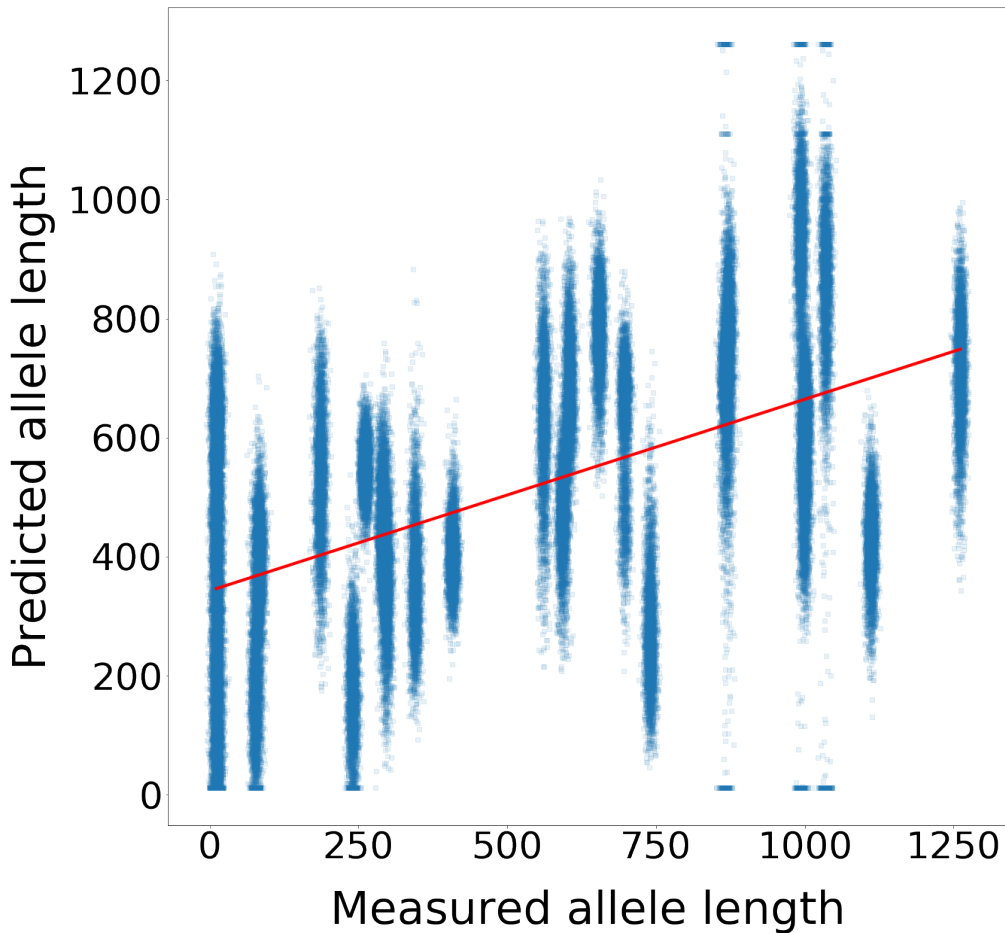


Fig 1. DM1-AS muscle MAL prediction. 10,000 repetitions of cross-validated MAL prediction from genes labeled DM1-AS from muscle for 18 training samples.

Other models

As described in [Data preparation and analysis](#), we have used a model based on feature selection from sets of candidate mRNA biomarkers to predict the MAL of DM1 CTG repeat using PLSR. As reported in [Performance of PLSR-based MAL predictors in muscle and blood](#), the set of genes DM1-AS is the strongest predictor if we limit our consideration to predictors chosen a-priori (*i.e.* excluding TNNI1).

A potential source of criticism could be that the effect observed is a technical effect due to the choice or the implementation of the mathematical model used (PLSR). We

thus re-ran the analysis as described before in [Data preparation and analysis](#) using three
311
mathematically distinct models: lasso, random forest regression and linear regression.
312

We report the performance of these models in Table 3:
313

Table 3. 10000 repetitions of a simulation predicting MAL from muscle, using DM1-AS as a predicting set and a selection of mathematical models

	linear regression	PLSR	lasso	random forest
R ²	0.291	0.289	0.286	0.149
p-value	0.00418	0.00434	0.00454	0.0478

It should be noted that all models pick up statistically significant signal with both
314
PLSR, lasso and linear regression performing almost equally well, and random forest
315
performing about two times poorer (but still significantly better than a random
316
predictor), which allows us to conclude that the effect observed is unlikely to be a
317
modelling artifact.
318

Applying the model in a clinical setting 319

Let us now consider the potential application of this predictive model in the context of
320
evaluating efficacy of a DM1 treatment. DM1 patients would undergo muscle biopsy
321
before starting the treatment, and another biopsy after the treatment had been started
322
and necessary biological changes to reverse DM1 symptoms had occurred. Both biopsies
323
would be mRNA profiled, and the resulting profiles would be used to perform MAL
324
predictions. We expect that pre-treatment prediction would correspond to the actual
325
MAL of any given participant. We expect that post-treatment prediction of MAL would
326
correspond to an “effective MAL”, which we would expect to be lower than the “actual
327
MAL” in affected participants, as long as the treatment is effective and DM1-induced
328
disruption of AS or APA, as measured by DM1-AS or DM1-APA biomarkers is
329
measurably reversed in obtained mRNA profiles. Pre-treatment and post-treatment
330
predictions could be combined into a statistic that, given enough patients, would allow
331
us to quantify the efficacy of the treatment at the molecular level. We discuss this idea
332
further in the chapter [Power Analysis](#).
333

In some respects, such a study could allow for better performance of the model,
334
conceptually, it should be easier to capture DM1 specific expression changes in a setting
335
where noise due to varied genetic backgrounds of participants can be reduced by looking
336

at pairs of measurements of a single participant. There are a number of details in such
337
study design, which need to be discussed by the community and decided upon, among
338
others:
339

1. The mathematical basis of the model used. We propose a PLSR-based model, and
340
demonstrate that models based on lasso and linear regression perform similarly,
341
but other models can also be considered, in particular the work of Azencott *et*
342
al. [16] in the context of L₁-penalised regression (lasso) looks promising as it
343
allows to incorporate prior biological knowledge, in the form of protein-protein
344
interaction networks or other types of graph ontology, into the model, through the
345
introduction of additional penalties based on discrete Laplacian, or apply
346
alternative modelling strategies based on network flow, thereby increasing its
347
predictive power.
348
2. The training/testing pre-treatment/post-treatment data split and which genes
349
should be included in the model input.
350
3. The size of the study. Predictions in our study are based on 24 participants for
351
blood and 18 for muscle. How much would the models' predictive power improve
352
with a larger dataset?
353
4. Establishing the clinically relevant effect size. Pandey *et al.* [7] report various
354
efficacies of a candidate DM1 treatment ISIS 486718 to lower toxic *DMPK*
355
concentrations in wild-type and transgenic animal models and a range of tissues,
356
starting with the efficacy of about 50% in cardiac muscle, through about 70% in
357
skeletal muscle, up to about 90% in liver and skeletal muscle. However, measuring
358
DMPK levels may not necessarily directly correspond to the efficacy of treatment
359
to reverse symptoms, as the relationship between the quantity of the toxic
360
transcript, splicing disruption and eventual clinical symptoms may be complex
361
and non-linear. Conservatively, we need to expect the rate of symptom reduction
362
to be lower than the reported 50% to 90%. A difficult open question is what
363
minimum treatment efficacy we are willing to accept as clinically significant?
364

An informal setting to explore the dataset

As this work is the first presentation of the DMBDI dataset, we recognise that further work might build on the dataset in ways which differ from our approach and cannot be predicted at the current stage of our understanding of DM1-related AS/APA changes. To facilitate this, we would like to propose a tool which on one hand allows for informal, interactive and exploratory analysis of the dataset and on the other allows the flexibility of building a custom analysis – just like the one presented here.

The tool is available online [23], and is implemented as a jupyter notebook with custom visualisation of filtered and normalised DMBDI data. The flexibility of the tool comes at a cost. In order to support arbitrary bioinformatics analyses we have to support arbitrary code execution, which in turn requires protecting the tool with a password. We will share the password with any bona fide researcher upon request. A walk-through video showcasing the capabilities of the tool is available on youtube [24].

The major capability of the tool is the ability to produce “railway plots”. Railway plots introduce the idea of a Manhattan plot from genomics community into transcriptomics. Each point represents statistical significance of the change of expression signal at a single probe across DM1 spectrum, as supported by experimental data. Points which belong to the same probeset, are identically coloured. See Figure 2 for an example railway plot.

In a railway plot the y-axis represents negative logs of p-values of a two-tailed tests against a null hypothesis of no expression change at a single probe across the DM1 spectrum. Figure 3 visualises one of such linear regressions for a probe belonging to probeset 245089. The logs of p-values are signed in accordance with the direction of the slope of the regression, with negative values indicating splice-out and positive values indicating a splice-in type of event.

For each of splice-out and splice-in directions in the plot, we show thresholds of statistical significance. The first pair of thresholds (faded red and blue respectively) correspond to statistical significance threshold of 0.05. The second pair of thresholds correspond to $0.05/n$, where n is the total number of probes in the plot (saturated red and blue respectively). This is analogous to the way Manhattan plots are often presented for GWAS.

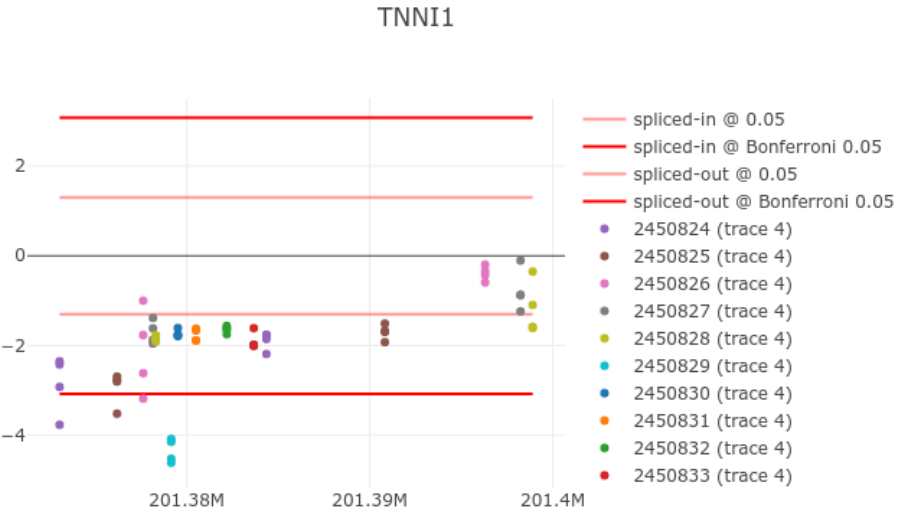


Fig 2. TNNI1 Railway plot shows an APA event at probeset 245089.

Turning our attention from statistics to biology, we can ask about a likely biological interpretation of an observed splice-out event detected at probeset 2450829. Using Ensembl [25], see figure 4), we can identify transcript TNNI1-203, which is the only GENCODE transcript featuring a probe selection region targeted by the probeset 2450829, in form of an alternative 3' UTR. This allows us to suggest that TNNI1-203 is downregulated in participants with longer DM1 repeats. GENCODE annotation further informs us that TNNI1-203 is an APPRIS P2 transcript (i.e. a candidate principal variant, a designation which comes from high level of support for functionality of the isoform), and is not a CDS incomplete transcript, which allows us to strengthen our belief in the fact that this is a biologically functional/ protein-coding transcript, which can play a role in the DM1-related AS/APA changes.

Finally, and returning back to statistics, we can ask whether high significance of the splice-out event is a result of multiplicity effect, given that the gene was chosen post-hoc from a pool of candidate biomarker genes as determined by Batra et al. and Nakamori et al. [8,9]. A standard approach here would be to combine the data from the discovery dataset with the data from the replication dataset, compute a more powerful test, and apply multiplicity correction. This is not possible in this case as the discovery dataset, underlying both studies is a case-control dataset, whereas our dataset captures DM1

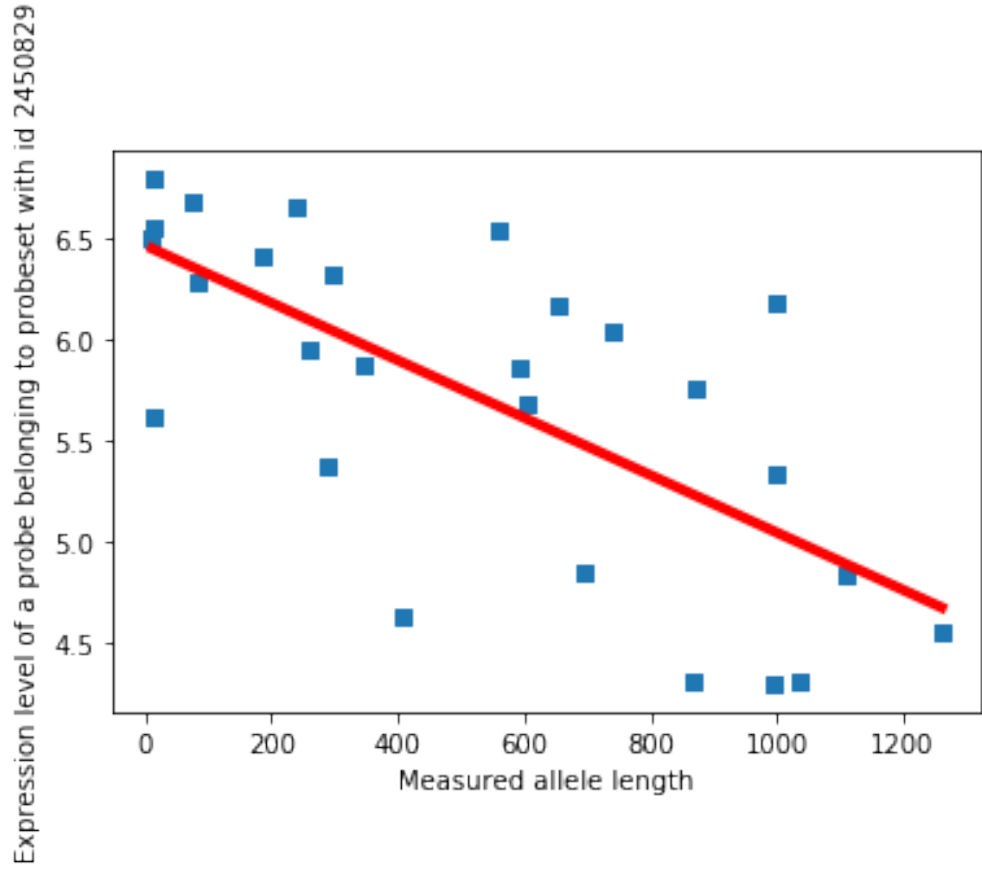


Fig 3. Linear regression of expression intensity at a single probe belonging to probeset 245089 against DM1 repeat length.

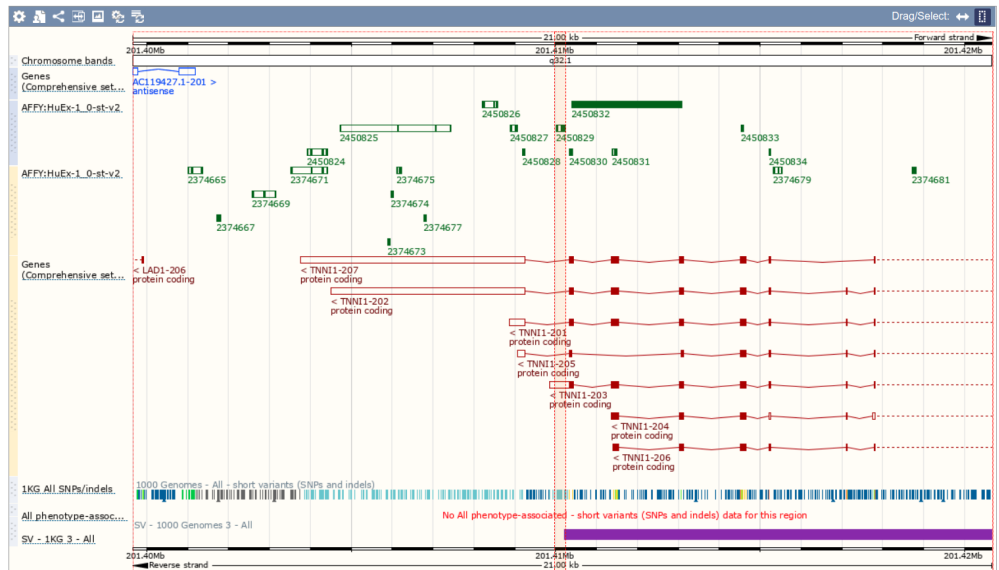


Fig 4. Visualisation of genomic coordinates of TNNI1 transcripts using Ensembl.

status as a continuous variable via DM1 CTG repeat length measurement. An 414 alternative is to combine both p-values using, e.g. Fisher's method [26], which shows 415 that the combined p-value against the null hypothesis of no change of signal intensity at 416 the probeset 2450829 is 4.19×10^{-10} . Computing the Bonferroni correction with 417 multiplicity factor of 1.4 million, equal to the total number of HuEx probesets [27], 418 shows that the combined p-value based on the discovery dataset and our dataset is 419 5.88×10^{-4} . This is a strong confirmation of the significant correlation of DM1 status 420 with TNNI1-203 downregulation. Details of the computation are available in S1 421 Appendix. 422

Power Analysis 423

Our final contribution, which is of critical significance in the context of any future 424 clinical trial is a power analysis of the current model. We report power for a selection of 425 possible treatment effect sizes (10%, 20% and 50% reduction in effective MAL on a 426 per-patient basis) and a selection of study participants. Our power is defined as $(1 - \beta)$, 427 where β is a supremum of the probability of committing a type II error, with the 428 supremum of the probability of committing type I error (α) kept at a constant 0.05. 429 Table 4 reports power, $(1 - \beta)$, to detect treatment effect of a two-tailed test with 430 p-value cut-off of 0.05 (0.025 per tail), with the statistic simulated from MAL 431 predictions of our model, for varying treatment effect and study sizes. We try to keep 432 our cohort sizes realistic for a rare disease, *i.e.* we allow for patient numbers to range 433 from 10 to 200. 434

Ideally we would like to be able to achieve power of more than 95%, even with small 435 treatment effect sizes and a small number of patients, but our model, trained on 18 436 participants, doesn't allow for such level of control over type II error for all but medium 437 or large treatment effects (more than 20% and 50% respectively) and large (more than 438 140 participants) or medium-sized (more than 30 participants) clinical trials respectively. 439

However, our results combined with expected improvements of the model 440 performance due to larger training samples, and better gene selections, such levels might 441 be reached for medium treatment effect size (20% reduction in effective MAL) and large 442 clinical sizes. 443

Table 4. Power analysis. Entries in the table report power to detect treatment effect based on the size of a cohort (from 10 – 200 participants) and the treatment effect of the study to reverse splicing changes (10, 20 and 50%). Entries denoting power greater than 0.95% are presented in boldface.

study size (participants)	treatment effect 10%	treatment effect 20%	treatment effect 50%
10	0.100	0.209	0.635
20	0.131	0.322	0.855
30	0.162	0.423	0.947
40	0.193	0.517	0.981
50	0.226	0.596	0.994
60	0.259	0.671	0.998
70	0.283	0.723	0.999
80	0.311	0.772	0.9998
90	0.339	0.816	0.99998
100	0.370	0.851	0.99999
110	0.396	0.881	0.99999
120	0.418	0.901	1.0
130	0.448	0.924	1.0
140	0.467	0.937	1.0
150	0.500	0.952	1.0
160	0.523	0.962	1.0
170	0.545	0.969	1.0
180	0.568	0.977	1.0
190	0.589	0.981	1.0
200	0.613	0.986	1.0

Limitations

A source of potential criticism is that muscles of DM1 patients have physiological differences (atrophy, increased fat content), especially when disease is severe. Quite possibly observed changes in AS/APA are partly attributable to these physiological differences in DM1 as opposed to purely biomolecular differences. The structure of this counter-argument could be as follows:

Muscles of DM1 patients have higher fat content than affected controls. Muscle samples collected from DM1 patients have higher ratio of intermuscular adipocytes to myocytes. Adipocytes have different AS/APA profiles than myocytes. Observed AS/APA changes in the DM1 spectrum are mostly derived from differences in adipocyte/myocyte profile. As a result, mRNA study of muscle tissue is no more effective (and possibly less effective) than a blinded study based on pathophysiological inspection of the tissue.

This argument can, of course, be extended to other physiological changes than increased fat content, and other molecular events than AS/APA. Bachinski et al. [28],

for example, propose that splicing changes could be a secondary result of muscle 459
regeneration. 460

There are multiple ways to address these concerns: 461

1. Alternative predictive model design based on tissue culture models, where *in vivo* 462
limitations are reduced, with homogeneity of the cellular composition of the model 463
being a big advantage. 464
2. Investigating methods to correct for potential “physiological” covariates (*e.g.* fat 465
content), using purely statistical techniques to estimate covariate influence from 466
gathered data and existing prior information (*e.g.* mRNA profiles of adipocytes), 467
or biological methods, such as a recent effort to collect higher quality muscle 468
samples through MRI-guided biopsy [29]. 469
3. Discovering DM1 biomarkers in blood, as opposed to muscle. Blood, being much 470
more homogeneous tissue than muscle is expected to be less prone to the existence 471
of confounding variables. Additionally, necessity of muscle sampling was 472
highlighted to be a “main drawback” [8]. However, achieving this would require at 473
least two separate, successful studies, one to identify biomarkers and one to 474
evaluate them. Even if blood biomarkers were identified, their clinical utility 475
might be limited, as a reduction of an effective MAL in blood would not be as 476
direct evidence of treatment effectiveness as such reduction in muscle. 477
4. Introduction of positive controls in experimental designs. Biological samples in 478
the positive control group would be composed of tissue collected from individuals 479
with other muscular dystrophies (*e.g.* Becker muscular dystrophy, Duchenne 480
muscular dystrophy, facioscapulohumeral muscular dystrophy or tibial muscular 481
dystrophy). These diseases feature dystrophy and increased muscle regeneration 482
program as part of their phenotype, but without disruption of RNA-binding 483
splicing factors. Absence of DM1-specific splicing changes in these positive 484
controls would allow to rule out alternative explanations of mis-splicing 485
mechanisms (*e.g.* muscle regeneration) and strengthen our belief in currently 486
accepted models of molecular pathomechanism of DM1. 487
5. Confining the analysis to transcripts which are exclusively or predominantly 488

expressed in skeletal muscle, not fat.

489

Conclusion

490

In this study we design and build a model based on PLSR, which can explain as much
491
as 28.9% of the variance in DM1 CTG trinucleotide expansion from mRNA splicing
492
data. Such explainability is only obtained when the model is trained on expression data
493
from genes previously identified by Nakamori *et al.* [8] as having disrupted AS on data
494
obtained from muscle samples. We show how such model could be used in a clinical
495
setting in the context of emerging DM1 treatments, and report power analysis to detect
496
treatment effect depending on size of the treatment effect, type 1 error (α) and
497
potential size of the clinical trial.

498

Supporting information

499

S1 Appendix. Code & how to run it. All of the computer programs written for
500
this study can be [found on github](#).
501

502

The following instructions should allow one to independently verify results of our
503
simulations (also available in the repository).

504

We advise that all of this code be run on a machine with 64 GB of RAM or more,
505
given that some parts of the pipeline can use up in excess of 32 GB of RAM. We were
506
able to successfully execute the entire analysis using an AWS “m5.4xlarge” EC2
507
instance. We found the default amount of storage, 8 GB, to be insufficient to store both
508
the primary data and intermediate computations. We increased the amount of storage
509
to 100 GB. We remove all networking restrictions on the instance, to allow for remote
510
access of jupyter notebooks, which contain our pipeline.

511

We had to apply the following shell commands to set up the machine:

512

1. sudo apt-get update
2. sudo apt-get upgrade
3. sudo apt-get install python3-pip
4. git clone https://github.com/picrin/clinical_applications.git

513

514

515

5. pip3 install jupyter

516

All data and metadata used in this study are available in publicly accessible s3
517
bucket, with the following paths: “dm1-biomarkers/CEL”,
518
“dm1-biomarkers/annotations” respectively. These datasets need to be copied to the root
519
of the “clinical_applications” repository as directories “CEL” and “annotations”
520
respectively.
521

521

All required third-party dependencies can be installed from the provided
522
“requirements.txt”
523

523

Finally, “jupyter notebook --ip 0.0.0.0 --port 8888” can be issued to start the
524
notebook server, which we can access remotely, using a DNS entry allocated for our
525
EC2 instance and provided that communications on our chosen port is configured to be
526
accessible through the AWS firewall.
527

527

We now run notebooks in the following order:
528

528

1. “01_parse_chip_data.ipynb”. This part of the pipeline is responsible for
529
determining probeset ids, sequences of probes and probe coordinates on the chip.
530
It produces an intermediate file with data adhering to the following schema:
531
“probeset, x, y, sequence”.
532
2. “02_parse_csv_annotations.ipynb”. Here, we determine “genomic” metadata, i.e.
533
chromosomal coordinates and strandedness.
534
3. “03_unpack_CEL_files.ipynb”. Here we use our own contribution to Biopython to
535
parse the binary CEL v4 file format, which is what all our microarray data uses.
536
4. “04_quantile_normalise.ipynb”. Here we perform quantile normalisation of our
537
microarray data.
538
5. “05_reannotate_probeset_level.ipynb”. Here we verify Affymetrix’s annotation. We
539
determine that over 1% probes are incorrectly annotated. We discard these
540
probes. We limit our attention to probes, which belong to chromosomes
541
chr1-chr22, X, Y and the mitochondrial DNA (M).
542
6. “06_intervaltrees.ipynb”. Here we carry out an exclusive filtering, choosing probes,
543
which are identified by “gencode.v26lift37.annotation.gtf” as having
544

“transcript_type” equal to “protein_coding”, or “gene_type” equal to 545
“protein_coding”, as well as the exon type equal to “CDS” (Coding sequence) or 546
“UTR” (5’ or 3’ untranslated regions). 547

7. “07_merge_annotation_experiment.ipynb”. Here we produce a single file per 548
human gene, as identified in GENCODE v26, with data from all participants for 549
all probes for that gene. 550

8. “08_predictions.ipynb”. Here we run our PLSR model to predict MAL from the 551
microarray data. 552

9. “10_power_analysis.ipynb”. Here we run power analysis presented in [Results & 553](#)
[Discussion](#). 554

10. “13_combine_p_values.ipynb”. Here we combine p-values for a probeset of interest 555
using a previously published p-value and one obtained in this study. 556

S2 Appendix. DM1-AS

ABLIM2, ALPK3, ANK2, ARFGAP2, ATP2A1, ATP2A2, BIN1, CACNA1S, 557
CAMK2B, CAPN3, CAPZB, CLCN1, COPZ2, DMD, DTNA, FHOD1, GFPT1, 558
IMPDH2, INSR, KIF13A, LDB3, MBNL1, MBNL2, MLF1, NFIX, NRAP, OPA1, 559
PDLIM3, PHKA1, RYR1, SOS1, TBC1D15, TTN, TXNL4A, UBE2D3, USP25, 560
VEGFA, VPS39 561

S3 Appendix. DM1-APA

ABCA1, AGL, ALG3, AMHR2, AP1G1, ARHGEF7, ASPH, ATP5E, BRSK2, 562
BRWD1, CACNA1G, CACNB1, CDC42, CEBPA, CELF1, CHRNA1, CIRBP, 563
CLDND1, COPS4, DAPK2, DES, DNAJB6, DST, DVL3, EZR, FASTK, GPS1, 564
HDAC11, IDH3A, ILF3, KCNK7, KDELR1, KIF1B, KRBA1, LAMP2, LDB3, LMNA, 565
MBNL2, MDN1, MEF2B, MEF2C, MEF2D, MGP, MORC3, MTCH1, MYH6, 566
NDUFB10, NR2F1, NUP43, OSBPL1A, PCBD2, PCM1, PCMT1, PDLIM2, PDLIM5, 567
PEBP4, PFKFB2, PIK3C2B, PLIN2, RAB24, RIN1, RTN2, SAMD4A, SETD3, 568
SLC25A36, SMIM3, SNX1, SPATS2L, SPEG, SPTB, TBL2, TGFBI, TJP2, 569
TMEM38B, TNNI1, TPM1, TPM2, TPM3, TTYH3, U2SURP 570

Acknowledgments

573

We would like to thank the Marigold Foundation for organising and funding DMBDI. 574

We would like to thank Linda Bachinsky and Keith Baggerly for their helpful 575
comments on multiple revisions of this manuscript, as well as performing initial analysis 576
and quality control on blood and muscle microarray samples. We would also like to 577
thank Anna Casasent (nee Unruh) for performing quality control on blood and muscle 578
microarray samples. 579

Adam Kurkiewicz would like to thank the college of Medical, Veterinary and Life 580
Sciences as well as the Engineering and Physical Science Research Council for financing 581
his doctoral training programme stipend, student fees and his research fund. 582

References

1. Brook JD, McCurrach ME, Harley HG, Buckler AJ, Church D, Aburatani H, et al. Molecular basis of myotonic dystrophy: Expansion of a trinucleotide (CTG) repeat at the 3' end of a transcript encoding a protein kinase family member. *Cell*. 1992;68(4):799–808. doi:10.1016/0092-8674(92)90154-5.
2. Meola G, Cardani R. Myotonic dystrophies: An update on clinical aspects, genetic, pathology, and molecular pathomechanisms. *Biochimica et Biophysica Acta (BBA) - Molecular Basis of Disease*. 2015;1852(4):594–606. doi:10.1016/j.bbadi.2014.05.019.
3. Thornton CA. Myotonic Dystrophy. *Neurologic Clinics*. 2014;32(3):705–719. doi:10.1016/j.ncl.2014.04.011.
4. Holt I, Jacquemin V, Fardaei M, Sewry CA, Butler-Browne GS, Furling D, et al. Muscleblind-Like Proteins. *The American Journal of Pathology*. 2009;174(1):216–227. doi:10.2353/ajpath.2009.080520.
5. Cudia P, Bernasconi P, Chiodelli R, Mangiola F, Bellocchi F, Russo AD, et al. Risk of arrhythmia in type I myotonic dystrophy: the role of clinical and genetic variables. *Journal of Neurology, Neurosurgery & Psychiatry*. 2009;80(7):790–793. doi:10.1136/jnnp.2008.162594.

6. Udd B, Krahe R. The myotonic dystrophies: molecular, clinical, and therapeutic challenges. *The Lancet Neurology*. 2012;11(10):891–905. doi:10.1016/s1474-4422(12)70204-1.
7. Pandey SK, Wheeler TM, Justice SL, Kim A, Younis HS, Gattis D, et al. Identification and Characterization of Modified Antisense Oligonucleotides Targeting DMPK in Mice and Nonhuman Primates for the Treatment of Myotonic Dystrophy Type 1. *Journal of Pharmacology and Experimental Therapeutics*. 2015;355(2):310–321. doi:10.1124/jpet.115.226969.
8. Nakamori M, Sobczak K, Puwanant A, Welle S, Eichinger K, Pandya S, et al. Splicing biomarkers of disease severity in myotonic dystrophy. *Annals of Neurology*. 2013;74(6):862–872. doi:10.1002/ana.23992.
9. Batra R, Charizanis K, Manchanda M, Mohan A, Li M, Finn DJ, et al. Loss of MBNL Leads to Disruption of Developmentally Regulated Alternative Polyadenylation in RNA-Mediated Disease. *Molecular Cell*. 2014;56(2):311–322. doi:10.1016/j.molcel.2014.08.027.
10. Bush WS, Moore JH. Chapter 11: Genome-Wide Association Studies. *PLoS Computational Biology*. 2012;8(12):e1002822. doi:10.1371/journal.pcbi.1002822.
11. Brody T. Biostatistics—Part I. In: *Clinical Trials*. Elsevier; 2016. p. 203–226. Available from: <https://doi.org/10.1016/b978-0-12-804217-5.00009-6>.
12. D'Agostino RB, Massaro JM, Sullivan LM. Non-inferiority trials: design concepts and issues - the encounters of academic consultants in statistics. *Statistics in Medicine*. 2002;22(2):169–186. doi:10.1002/sim.1425.
13. du Prel JB, Röhrig B, Hommel G, Blettner M. Choosing Statistical Tests. *Deutsches Aerzteblatt Online*. 2010;doi:10.3238/ärztebl.2010.0343.
14. Lello L, Avery SG, Tellier L, Vazquez A, de los Campos G, Hsu SDH. Accurate Genomic Prediction Of Human Height. *bioRxiv*. 2017;doi:10.1101/190124.
15. VanRaden PM, Tassell CPV, Wiggans GR, Sonstegard TS, Schnabel RD, Taylor JF, et al. Invited Review: Reliability of genomic predictions for North American

Holstein bulls. *Journal of Dairy Science*. 2009;92(1):16–24. doi:10.3168/jds.2008-1514.

16. Azencott CA, Grimm D, Sugiyama M, Kawahara Y, Borgwardt KM. Efficient network-guided multi-locus association mapping with graph cuts. *Bioinformatics*. 2013;29(13):i171–i179. doi:10.1093/bioinformatics/btt238.
17. Lee JM, Galkina EI, Levantovsky RM, Fossale E, Anderson MA, Gillis T, et al. Dominant effects of the Huntington's disease HTT CAG repeat length are captured in gene-expression data sets by a continuous analysis mathematical modeling strategy. *Human Molecular Genetics*. 2013;22(16):3227–3238. doi:10.1093/hmg/ddt176.
18. Monckton DG, Wong LJC, Ashizawa T, Caskey CT. Somatic mosaicism, germline expansions, germline reversions and intergenerational reductions in myotonic dystrophy males: small pool PCR analyses. *Human Molecular Genetics*. 1995;4(1):1–8. doi:10.1093/hmg/4.1.1.
19. Morales F, Couto JM, Higham CF, Hogg G, Cuenca P, Braida C, et al. Somatic instability of the expanded CTG triplet repeat in myotonic dystrophy type 1 is a heritable quantitative trait and modifier of disease severity. *Human Molecular Genetics*. 2012;21(16):3558–3567. doi:10.1093/hmg/dds185.
20. Rexiati M, Sun M, Guo W. Muscle-Specific Mis-Splicing and Heart Disease Exemplified by RBM20. *Genes*. 2018;9(1):18. doi:10.3390/genes9010018.
21. Cock PJA, Antao T, Chang JT, Chapman BA, Cox CJ, Dalke A, et al. Biopython: freely available Python tools for computational molecular biology and bioinformatics. *Bioinformatics*. 2009;25(11):1422–1423. doi:10.1093/bioinformatics/btp163.
22. Kurkiewicz A. Parser for Affy CEL file version 4; 2016. Available from: <https://github.com/biopython/biopython/commit/6c14a26dda32ad6d3147036a01f3d0c4d306c647>.
23. Kurkiewicz A. DMBDI explorer; 2019. Available from: <http://dmbdi.adamkurkiewicz.com>.

24. Kurkiewicz A. DMBDI explorer walk-through video; 2019. Available from: <https://youtu.be/gvs5XtdYwE0>.
25. Kersey PJ, Allen JE, Allot A, Barba M, Boddu S, Bolt BJ, et al. Ensembl Genomes 2018: an integrated omics infrastructure for non-vertebrate species. *Nucleic Acids Research*. 2017;46(D1):D802–D808. doi:10.1093/nar/gkx1011.
26. Fisher RA. Statistical Methods for Research Workers. Oliver and Boyd; 1934.
27. Affymetrix. GeneChip® Exon Array Design; 2005. Available from: http://tools.thermofisher.com/content/sfs/brochures/exon_array_design_technote.pdf.
28. Bachinski LL, Baggerly KA, Neubauer VL, Nixon TJ, Raheem O, Sirito M, et al. Most expression and splicing changes in myotonic dystrophy type 1 and type 2 skeletal muscle are shared with other muscular dystrophies. *Neuromuscular Disorders*. 2014;24(3):227–240. doi:10.1016/j.nmd.2013.11.001.
29. Lassche S, Janssen BH, IJzermans T, Fütterer JJ, Voermans NC, Heerschap A, et al. MRI-Guided Biopsy as a Tool for Diagnosis and Research of Muscle Disorders. *Journal of Neuromuscular Diseases*. 2018;5(3):315–319. doi:10.3233/JND-180318.